

Castration-resistant prostate cancer bone metastasis response measured by ¹⁸F-fluoride PET after treatment with dasatinib and correlation with progression-free survival: Results from ACRIN 6687

Authors: Evan Y. Yu,^{1*} Fenghai Duan,² Mark Muzi,¹ Xuan Deng,² Bennett B. Chin,³ Joshi J. Alumkal,^{4*} Mary-Ellen Taplin,^{5*} Jina M. Taub,¹ Ben Herman,² Celestia S. Higano,^{1*} Robert K. Doot,⁶ Donna Hartfeil,⁷ Philip G. Febbo,^{8*} and David A. Mankoff⁶

Affiliations: ¹University of Washington, Seattle, WA; ²Department of Biostatistics and Center for Statistical Sciences, Brown University School of Public Health, Providence, RI; ³Duke University, Durham, NC; ⁴Oregon Health & Science University, Portland, OR; ⁵Dana-Farber Cancer Institute, Boston, MA; ⁶University of Pennsylvania, Philadelphia, PA; ⁷American College of Radiology Imaging Network (ACRIN), Philadelphia, PA; ⁸University of California San Francisco, San Francisco, CA

*These authors are members of the Prostate Cancer Clinical Trials Consortium, sponsored by the Department of Defense

Corresponding author:

Evan Y. Yu, M.D.

Division of Oncology

Department of Medicine

University of Washington School of Medicine

825 Eastlake Avenue East, G4-836

Box 358081

Seattle, WA 98109

Tel: 206-288-7595

Fax: 206-288-2042

Email: evanyu@uw.edu

Word count: 5397

Research support: NIH U01 CA080098 (ARRA 2009), U01 CA079778, and
Bristol-Myers Squibb

Running title: CRPC response by ^{18}F -fluoride PET

ABSTRACT

¹⁸F-fluoride PET quantitatively images bone metabolism and may serve as a pharmacodynamic assessment for systemic therapy like dasatinib, a potent SRC kinase inhibitor, with activity in bone.

Methods

This was an imaging companion trial (ACRIN 6687) to a multi-center metastatic castration-resistant prostate cancer (mCRPC) tissue biomarker-guided therapeutic trial (NCT00918385). Men with bone mCRPC underwent ¹⁸F-fluoride PET prior to and 12 weeks after initiation of dasatinib 100 mg daily. Dynamic imaging was performed over a 15 cm field of view for trial assessments. The primary endpoint was to determine if changes in ¹⁸F-fluoride incorporation in tumor and normal bone occur in response to dasatinib. Other endpoints included differential effect of dasatinib between ¹⁸F-fluoride incorporation in tumor and normal bone, ¹⁸F-fluoride transport in bone metastases, correlation with progression-free survival (PFS), prostate-specific antigen and markers of bone turnover.

Results

Eighteen participants enrolled and 17 had interpretable baseline ¹⁸F-fluoride PET imaging prior to initiation of dasatinib. Twelve of 17 patients underwent on-treatment PET imaging. Statistically significant changes in response to dasatinib were identified by standardized uptake value (SUV)_{maxavg} in bone metastases (p=0.0002) with a significant differential ¹⁸F-fluoride PET response between tumor and normal bone (p<0.0001). Changes in ¹⁸F-fluoride incorporation in bone

metastases had borderline correlation with PFS by SUV_{maxavg} (HR=0.91, 95% CI 0.82-1.00; $p=0.056$). Changes by SUV_{maxavg} correlated with bone alkaline phosphatase ($p=0.0014$) but not PSA ($p=0.47$).

Conclusions

This trial provides evidence of ^{18}F -fluoride PET ability to delineate treatment response of dasatinib in CRPC bone metastases with borderline correlation with PFS.

Keywords: ^{18}F -fluoride PET, bone metastases, dasatinib, metastatic castration-resistant prostate cancer

INTRODUCTION

Determination of therapeutic response in prostate cancer bone metastases is challenging as traditional imaging relies on measuring changes in bone turnover with bone scintigraphy or bone structure with computed tomography (CT) or magnetic resonance imaging (MRI). However, these imaging modalities are limited by a lack of quantitative ability. Prostate-specific antigen (PSA) decline is also utilized as a treatment response measure, however, PSA does not differentiate variability in tumor response across different disease sites. PET imaging is inherently quantitative and offers regional measures of both *in vivo* tumor and normal tissue biology using tracers for glucose, lipid, or bone metabolism, among other processes. ^{18}F -FDG is a radioactive tracer utilized in routine PET imaging for many malignancies, but it generally lacks sensitivity for imaging osteoblastic prostate cancer lesions (1).

^{18}F -fluoride offers a quantitative measure of new bone formation and turnover in both normal bone and bone metastases, making it well-suited for blastic lesions (2, 3). Recent studies with ^{18}F -fluoride PET show improved sensitivity over bone scintigraphy for multiple solid tumors, including prostate cancer (2, 4). Therefore, ^{18}F -fluoride PET offers the ability to image metastatic lesions with excellent sensitivity while offering quantitative capability for measuring treatment response, especially for therapeutics with bone remodeling effects such as dasatinib (5-8).

Dasatinib (SPRYCEL[®]; Bristol-Myers Squibb) is an oral tyrosine kinase inhibitor with potent activity against the Src Family Kinases (SFKs), BCR-ABL,

PDGFR and c-KIT (9). SFKs are overexpressed in prostate cancer and SRC inhibition results in reduced cancer cell proliferation, invasion, and migration (10, 11). Furthermore, SFKs play an important role in osteoclast and osteoblast function, with SRC inhibition delaying the appearance and decreasing the size of bone metastases in murine models of breast cancer (12, 13). Dasatinib treatment of orthotopic murine bone prostate tumor models have demonstrated decreased PSA, increased bone mineral density, decreased serum calcium, and potentiated docetaxel chemotherapy effects (14). Phase 2 trials in patients with metastatic castration-resistant prostate cancer (mCRPC) showed significant decreases in bone turnover markers (15, 16). An open-label combination phase 1-2 trial with a dasatinib/docetaxel combination also confirmed significant bone turnover activity with impressive anti-tumor effect (17). In a randomized, placebo-controlled, phase 3 trial, an overall survival (OS) benefit could not be confirmed with the dasatinib/docetaxel combination over placebo/docetaxel, yet time to first skeletal-related event (SRE) was in favor of patients who received dasatinib (HR 0.81, 95% CI 0.64-1.02, p=0.08) (18). The discrepancy between clear activity of dasatinib in bone and anti-tumor endpoints such as OS raises the question whether the activity of dasatinib is primarily as an osteoclast inhibitor in normal bone, or whether there is preferential activity on bone metastases.

This imaging trial sought to determine comparative pharmacodynamic effect of dasatinib in normal bone and bone metastases. Given expression of SRC both in osteoclasts and in prostate cancer, and the observed clinical activity on bone turnover markers, ¹⁸F-fluoride PET, as a quantitative imaging method

targeted to bone, was ideally suited for this purpose. Therefore, patients were imaged with ¹⁸F-fluoride PET/CT both at baseline and 12 weeks after initiation of dasatinib to determine if the nature of the drug effect could be ascertained by imaging. Specifically, can ¹⁸F-fluoride PET/CT discern dasatinib response in normal bone and bone metastases and identify a preferential drug effect in the tumor? An exploratory aim was to test the ability of ¹⁸F-fluoride PET to measure clinical outcomes with dasatinib, assessed by progression-free survival (PFS).

MATERIALS AND METHODS

Study Design and Treatments

ACRIN 6687 was a phase 2 trial conducted by the American College of Radiology Imaging Network (ACRIN) at 4 Prostate Cancer Clinical Trials Consortium centers: University of Washington, Duke University, Oregon Health Sciences University and the Dana-Farber Cancer Institute (NCT00936975). Men with mCRPC were administered dasatinib 100 mg orally QD on a phase 2 companion clinical trial (NCT00918385). This trial selected patients for dasatinib based on a metastatic biopsy and determination of a 300-gene androgen receptor (AR) signature. Patients initially found to have an AR high (gene expression \geq median) signature received nilutamide with dasatinib added at progression. Patients with an AR low/SRC high signature (19), were treated initially with dasatinib. Patients receiving dasatinib underwent ¹⁸F-fluoride PET both at baseline and again 12 +/-4 weeks after initiation of dasatinib (Figure 1). This time point for PET imaging was selected both from prior published bone

biomarker data (15, 16) with dasatinib and to match with CT and bone scans from the therapeutic trial.

Patient Eligibility

This trial was reviewed and approved by the institutional review board of all participating sites, and all patients signed written informed consent before commencement of study procedures.

Key inclusion criteria for this trial included: males age ≥ 18 years with histologically or cytologically proven prostate carcinoma, radiologic evidence of metastatic bone disease and either biochemical, radiographic or symptomatic progression of mCRPC with maintained castrate serum testosterone levels (< 50 ng/dL). Required treatment withdrawal time frames for were: 30 days from anti-androgens prior to baseline PSA, 4 weeks from radiation or radiopharmaceutical treatment to bone, and 4 weeks from granulocyte-macrophage colony stimulating factor (GM-CSF) or G-CSF prior to first PET scan. Other requirements included adequate organ function and an ECOG performance status 0–2 with life expectancy ≥ 12 weeks.

Key exclusion criteria included: prior receipt of either nilutamide or dasatinib or amiodorone, lack of recovery to grade ≤ 1 toxicity from prior therapy, history of major cardiac condition, uncorrected hypokalemia or hypomagnesemia, clinically significant pleural or pericardial effusion, severe respiratory insufficiency, or any other uncontrolled intercurrent illness. Directly relevant to PET imaging, patients with poor intravenous access, weight > 300 lbs due to

equipment specifications or those with inability to lie still for imaging were also excluded.

Imaging Protocol and Analysis

All PET imaging scanners were pre-qualified by the ACRIN Imaging Core Laboratory using phantom scans with known activity and sample patient image sets were submitted for qualitative review and approval. PET imaging data was acquired using either a GE Discovery STE (n=24 scans) or a Seimens Biograph 16 (n=2 scans). After careful consideration of the anticipated biologic impact of therapy with dasatinib on fluoride delivery and vasculature, dynamic imaging, limiting us to a single 15 cm field of view (FOV), was considered essential. The lead nuclear medicine physician from the local study site reviewed both bone and CT scans to identify the most prominent metastasis site for the dynamic FOV, Regions in the upper abdomen and thorax were preferred to capture a blood clearance curve from the heart or aorta. A low dose CT transmission scan was acquired for attenuation correction, after which a 5.18 MBq/kg intravenous injection of ^{18}F -fluoride (mean dose 329 MBq, range 282 to 370 MBq) was administered over 1 minute. At the onset of tracer injection a 60-minute dynamic 3D acquisition imaging protocol (16x5 sec, 7x10 sec, 5x30 sec, 5x60 sec, 5x3 min, 7x5 min) was initiated. A static whole body image from mid-thigh to head was then obtained for attenuation correction, and a torso survey with emission scanning was performed at imaging times of 2-5 minutes per position depending upon the scanner. Image reconstruction corrected for attenuation, decay, scatter, and random coincidences, using the scanner manufacturers method of 3D

reconstruction. DICOM header information for each image series was vetted against ACRIN form information completed by local sites at the time of scanning. All images were sent to the ACRIN imaging core lab at the University of Washington for central imaging review. The data presented here are based upon analysis of the dynamic imaging data; analysis of the static whole-body survey images will be the subject of a future analysis.

Image Analysis

Dynamic imaging data served as the primary imaging endpoint in this trial. A subset of the dynamic imaging data (30-60 min SUV) were summed and reconstructed, and used to create volumes of interest (VOI) for data extraction and modeling. Using both the CT and static summed PET emission images, VOIs were constructed on up to 5 lesions with the greatest ^{18}F uptake in the dynamic FOV. In the tumor VOI construction procedure, a 1cc VOI was centered over the region of maximum tumor intensity, on the pixel with the maximum value. Tumor-matched normal bone regions, identified by both CT and ^{18}F -fluoride PET, of identical volume were also constructed. SUV and SUV_{max} values for each region were obtained from the 30-60 min static summed SUV image, while time course data were extracted from the dynamic PET series as tissue time-activity curves (TACs). SUV_{max} was defined as the SUV for the voxel within the tumor VOI with the maximal uptake. $\text{SUV}_{\text{maxavg}}$ was the average of SUV_{max} for up to 5 tumors within the dynamic FOV. To acquire a blood input function for compartmental modelling analysis, a 1 cm diameter cylindrical VOI was

constructed on the CT image set covering at least 3 cm of the aorta and applied to the dynamic PET series to extract an image-derived blood TAC.

Compartmental Modelling

The 2-tissue compartment kinetic model of fluoride metabolism of Hawkins (5), as modified by Doot (7) was used for parameter optimization of the dynamic ^{18}F tissue TACs using the blood TAC as input to the model. The transfer from blood into tissue is represented by K_1 , while the return of ^{18}F from a tissue compartment representing un-bound ^{18}F back to blood is represented by k_2 . The metabolic trapping of ^{18}F through new bone formation is represented by k_3 , which is the rate limiting step for the intracellular trapping of ^{18}F in bone. There is some evidence that ^{18}F can leave the imaging region by bone degradation back to ^{18}F and subsequent efflux. The loss of image signal through these processes is adequately described by k_4 .

The ^{18}F flux is estimated through compartmental model optimization, which fits model parameters to the tissue TAC data using the ^{18}F blood activity curve as the input function in a software package designed for PET data analysis (PMOD v3.408, PMOD group, Zurich, Switzerland). The ^{18}F flux constant, K_i , is determined by the product of the rates of ^{18}F metabolism ($K_i = (K_1 \cdot k_3) / (k_2 + k_3)$) and represents the rate of ^{18}F trapping as a quantitative measure of new bone and fluoride deposition (5, 7). The key parameters for describing ^{18}F uptake in tissue are the ^{18}F blood-tissue transport rate, K_1 , and the flux constant, K_i .

Study Endpoints

The primary study endpoint was to determine if changes in regional fluoride incorporation, measured by ^{18}F -fluoride PET, occur in both CRPC bone metastases and normal bone in response to treatment with dasatinib. This was determined, as described above, within the 15 cm dynamic FOV by both SUV_{max} and K_i , an indicator of net plasma clearance of fluoride to bone mineral. The secondary endpoint of the trial determined if changes in ^{18}F -fluoride transport, K_1 , an indicator of blood flow, and therefore, an indirect marker of angiogenesis, occurred in both CRPC bone metastases and normal bone in response to treatment with dasatinib. As a pre-specified exploratory analysis, the difference of dasatinib treatment effects by SUV_{max} , K_i and K_1 in normal bone was subtracted from the difference in these measures in tumor bone.

Other exploratory efficacy endpoints compared ^{18}F -fluoride parameters of SUV_{max} , K_i and K_1 in bone metastases at baseline and change in response to treatment with dasatinib directly with PFS, as defined by the Prostate Cancer Working Group 2 (PCWG2) (20). Additionally, changes in SUV_{max} , K_i and K_1 , in response to dasatinib treatment, were compared with changes in urinary N-telopeptide (uNTX), bone alkaline phosphatase (BAP) and PSA.

Statistical Analyses

Based on data reported by Frost et al (6), where ^{18}F -fluoride PET found a 15.6% decrease in K_i from baseline to 6-month post-bisphosphonate scan, this trial was powered to detect a more modest 10% change in K_i or SUV_{max} from baseline to post-treatment scan. Under these assumptions, 24 patients were

required to achieve a 0.05 target significance level and 80% power using a two-sided paired t-test to compare pre- and post-treatment measurements at the patient level.

The mean value of the change from pre- to post-dasatinib treatment was calculated to represent the patient-level change for each uptake parameter (i.e., SUV_{maxavg} , K_{iavg} , K_{1avg}). To test if the changes were statistically significant, the generalized estimating equation (GEE) was fitted to analyze the bone-level data after adjusting for clustering of data within subjects. Specifically, the compound symmetry was used to denote the correlations among measurements collected from the same patient.

The association between changes of these parameters and PFS was evaluated via Cox proportional hazards models. This was done under a univariate setting due to the limitation of sample sizes and lack of degree of freedom to adjust for other covariates. Spearman rank correlation was used to examine correlations between changes in SUV_{maxavg} , K_{iavg} , and K_{1avg} and changes in PSA and markers of bone turnover, BAP and uNTX.

RESULTS

Patients and Treatment

Between September 2009 and November 2010, 18 patients were enrolled in the trial. The goal was 24 patients, however, the companion therapeutic clinical trial (NCT00918385) closed to accrual prematurely due to regulatory issues surrounding the biopsy genetic signature. Since this imaging trial related only to

patients receiving dasatinib, the regulatory issues did not affect this data, analysis or results, other than limiting the number of patients accrued. Of the 18 patients enrolled, all underwent baseline ^{18}F -fluoride PET imaging. One patient had PET data that was not interpretable due to technical issues. Thirteen of these 17 patients underwent the second PET imaging 12 +/-4 weeks after initiation of dasatinib. Four patients suffered from early clinical progression and were removed from the trial prior to receiving the on-treatment second PET scan. Another patient had PET data from the second scan that was not interpretable due to technical issues. Therefore, 12 patients were evaluable to assess response to dasatinib treatment endpoints. Patient characteristics and demographic data are presented in Table 1. Median followup for the 17 patients with interpretable baseline scans and for the 12 patients evaluable for treatment response was 452 (range 76-815) and 455 (167-645) days, respectively.

^{18}F -fluoride as a Pharmacodynamic Measure of Dasatinib

A total of 37 pairs of tumor and normal bones were identified from the 12 patients who had both evaluable pre- and post-dasatinib PET images. To assess the primary endpoint of change in fluoride incorporation into bone, both SUV_{max} and K_i were evaluated. Changes in bone metastases in response to dasatinib by SUV_{max} were notable with -6.61 decrease of $\text{SUV}_{\text{maxavg}}$ (95% CI: -10.07, -3.15, $p=0.0002$) versus null hypothesis of no change from GEE) (Figure 2, top panel). No significant changes in SUV_{max} of normal bone sites were noted with +0.33 increase in $\text{SUV}_{\text{maxavg}}$ (95% CI: -0.32, 0.97, $p=0.32$). Changes by K_i were not significant in either tumor or normal bone (Figure 2, middle panel).

Since SRC inhibition has been shown to potentially decrease angiogenesis (21), the secondary endpoint of the trial was to evaluate the effect of dasatinib in bone metastases and normal bone on ^{18}F -fluoride PET radiotracer flow (K_1). Changes in bone metastases and normal bone in response to dasatinib by K_1 were not significant (Figure 2, bottom panel).

A key endpoint of the trial was to determine if there is a differential response between tumor and normal bone (Figure 2). This was significant for SUV_{max} with a difference of -6.98 (95% CI: -10.30, -3.66, $p < 0.0001$). There was no differential response between tumor and normal bone by K_1 . Although previously, there was no difference in K_1 in response to treatment with dasatinib by either tumor or normal bone, there is a trend towards significance in the differential response between tumor and normal bone with an absolute change of -0.04 (95% CI: -0.082, 0.0002, $p = 0.051$).

Associations Between ^{18}F -fluoride PET and PFS

As exploratory endpoints, both baseline PET parameters and change in response to dasatinib by ^{18}F -fluoride PET in bone metastases were compared with PCWG2-defined PFS. All patients developed progression and were evaluable for PFS, therefore $n = 17$ for baseline PET parameters and $n = 12$ for change from baseline to post-dasatinib PET. PFS was measured from the initiation of dasatinib to an event or censoring.

Results of the PFS association analysis are presented in Table 2. Other parameters such as Gleason, PSA, uNTX and BAP were also evaluated, and although baseline PSA, uNTX and BAP had association with PFS, changes in

these parameters did not correlate with PFS. Although baseline SUV_{maxavg} , K_{iavg} , and K_{1avg} did not correlate with PFS, changes in response to treatment with dasatinib has borderline correlation with PFS for SUV_{maxavg} (HR 0.91, 95% CI 0.82-1.00; $p=0.056$). Interestingly, the HR was <1 implying that patients with smaller decreases or even increases in uptake of ^{18}F -fluoride had longer PFS, rather than shorter PFS. For detailed granularity, individual change in SUV_{maxavg} in relation to PFS is shown in Figure 3. This finding was contradictory our original hypothesis and will be further addressed below in the discussion.

^{18}F -fluoride PET Correlation with Bone Biomarkers and PSA

Other exploratory endpoints compared changes in ^{18}F -fluoride PET parameters in response to dasatinib in bone metastases with changes in PSA and bone biomarkers (Table 3). Specifically, change in BAP had a significant negative correlation with change ^{18}F -fluoride PET by SUV_{maxavg} . Change in uNTX and PSA had no correlation with changes by ^{18}F -fluoride PET.

DISCUSSION

Prostate cancer clinical research is challenged by lack of validated disease response endpoints for bone metastases. Bone scintigraphy is not a quantitative measure and response to therapy is impossible to describe outside of the detection of new lesions. As a result, prostate cancer trials have focused on endpoints such as OS and radiographic PFS, rather than response to therapy (20). These endpoints require significant patient numbers and follow-up and may

not be practical for widespread use in the clinic due to inability to offer a real-time assessment of treatment response to the patient.

For these reasons, we embarked on this multicenter, cooperative group, prospective imaging biomarker trial to determine response to therapy by PET. The selection of ^{18}F -fluoride as the radiotracer was a purposeful coupling with a bone-dominant disease and a therapeutic agent with effects in bone. The goal of demonstrating bone metastatic changes in response to dasatinib and differential change for normal bone compared to bone metastases was successfully demonstrated. Specifically, there was a significant difference in the change in ^{18}F -fluoride $\text{SUV}_{\text{maxavg}}$ with dasatinib for bone metastases versus normal bone, with bone metastases, but not normal bone, having a significant decline in uptake. To lend this finding further credence, we confirmed that changes ^{18}F -fluoride uptake in bone metastases correlated with accepted criteria for radiographic PFS.

It is perhaps surprising that K_i was not a better indicator of ^{18}F -fluoride incorporation than SUV_{max} or $\text{SUV}_{\text{maxavg}}$, however, we noted anecdotally that the ^{18}F -fluoride curves had statistical noise, suggesting more limited precision in the kinetic estimates. SUV measures reporting the hottest pixel from a high resolution 30 min image showed less variation than a 1cc VOI from a tumor region that may include a distribution of voxels over a wide range of intensity levels. Correcting for partial volume effect or segmenting the tumor volume may have helped reduce the variability. This will require further study and confirmation in more detailed analyses.

We were surprised at the nature of the borderline correlation found between changes in ^{18}F -fluoride incorporation by PET and PFS. Notably, patients with the largest decrease in radiotracer incorporation in bone in response to dasatinib had the worst outcomes, which were unexpected for predominantly blastic prostate cancer bone metastases, where we might expect treatment to decrease blastic activity at the site of metastasis. Those with a lower decline or even an increase in blastic activity, had the longest durations until progression. Dasatinib has been shown previously to promote osteoblast differentiation (22) and mineralization that could lead to a relative activation and increase in bone mineralization, somewhat similar to osteoblast activation accompanying a healing “flare” seen on bone scan and ^{18}F -fluoride PET (23), where early increases in uptake, indicative of a healing or reparative response, may occur in patients with PSA declines and/or other evidence of response to systemic therapy. Further mechanistic studies will be needed to test this hypothesis and rule out the possibility that this finding was obtained by chance.

Although not a validated endpoint for drug approval, PSA is commonly utilized in the clinic to assess response to therapy. Dasatinib has had minimal effect on PSA in early clinical trials (15, 16), and given the mechanism of action on SRC, it might not be expected to have as much effect on PSA as agents that inhibit the androgen axis. Nevertheless, we evaluated correlation between PSA with ^{18}F -fluoride PET parameters and found none, e.g., $\text{SUV}_{\text{maxavg}}$ ($p=0.47$), K_{avg} ($p=0.49$), and $\text{K}_{1\text{avg}}$ ($p=0.64$).

Our trial had a number of limitations. Selection (or attrition) bias introduced by informative censoring is a common issue for cancer treatment trials with PFS as the study endpoint (24). Another potential bias could result from the 4 patients who exited the trial due to rapid disease progression before the second on-treatment PET study. Therefore, findings of this trial are limited to those patients with disease indolent enough to allow acquisition of a second on-treatment PET scan. Unfortunately, the small sample size precluded application of efficient methods to correct for these types of biases or to perform multivariable analyses. A number of variables were evaluated as potential predictors of radiographic PFS, therefore, the borderline correlations between SUV_{maxavg} and radiographic PFS could be due to chance. Finally, the timing for the second ^{18}F -fluoride PET scan had a large window to accommodate the complexity of the therapeutic trial, and this may have contributed some variability in findings.

Heterogeneity of ^{18}F -fluoride PET radiotracer uptake, and heterogeneity of changes in response to dasatinib treatment were observed (Figure 4). This heterogeneity is not surprising, as prostate cancer has been demonstrated to have significant diversity from one metastasis to another (25, 26). The ability to identify such heterogeneity emphasizes one of the strengths of PET imaging, as PSA only offers a summed overview and molecular characterization by biopsy and assay of a metastasis only offers data from that specific lesion. Given the mechanism of action of dasatinib, it was felt that certain dynamic measures such as K_i and K_1 might effectively capture the biologic activity of the drug. For this reason, we were limited in analysis to the dynamic FOV, and it is possible that

important data outside the dynamic FOV may not have been captured. Although outside of the scope of this manuscript, more information may be gained by evaluating the whole-body static surveys, and this future analysis will focus on heterogeneity of disease response.

Larger trials must be performed to confirm the interesting findings in this small, prospective trial. Although the development of dasatinib is unlikely to proceed as a prostate cancer therapeutic, imaging biomarker studies of this sort may help future development of novel agents by offering pharmacodynamic assessments to aid in selection of patients most likely to benefit. Other ^{18}F -fluoride PET trials are underway, and it is now being tested with current standard of care agents (NCT01516866).

CONCLUSION

^{18}F -fluoride PET is capable of identifying dasatinib treatment response in CRPC bone metastases and these changes may correlate with PFS. Validation of these findings from larger, prospective trials with other therapeutic agents is required.

DISCLOSURES:

Evan Y. Yu: Research – Bristol-Myers Squibb

Fenghai Duan: Paid Consultant - WorldCare Clinical, LLC

ACKNOWLEDGMENTS

The study was supported by ACRIN, which receives funding from the National Cancer Institute through U01 CA080098, under the American Recovery and Reinvestment Act of 2009 (ARRA), U01 CA079778, and Bristol-Myers Squibb. Imaging analysis was supported by the Quantitative Imaging Network U01 CA148131. All patients were accrued at DoD Prostate Cancer Clinical Trials Consortium (UW W81XWH-09-1-0144, Duke W81XWH-09-1-0152, OHSU W81XWH-09-1-0140, DFCI W81XWH-09-1-0150) and Prostate Cancer Foundation Therapy Consortium sites.

REFERENCES

1. Cook GJ, Fogelman I. Detection of bone metastases in cancer patients by ^{18}F -fluoride and ^{18}F -fluorodeoxyglucose positron emission tomography. *Q J Nucl Med* 2001;45:47-52.
2. Beheshti M, Langsteger W, Fogelman I. Prostate cancer: role of SPECT and PET in imaging bone metastases. *Semin Nucl Med* 2009;39:396-407.
3. Schoder H, Larson SM. Positron emission tomography for prostate, bladder, and renal cancer. *Semin Nucl Med* 2004;34:274-292.
4. Schirrmester H, Guhlmann A, Elsner K, et al. Sensitivity in detecting osseous lesions depends on anatomic localization: planar bone scintigraphy versus ^{18}F PET. *J Nucl Med* 1999;40:1623-1629.
5. Hawkins RA, Choi Y, Huang SC, et al. Evaluation of the skeletal kinetics of fluorine-18-fluoride ion with PET. *J Nucl Med* 1992;33:633-642.
6. Frost ML, Cook GJ, Blake GM, Marsden PK, Benatar NA, Fogelman I. A prospective study of risedronate on regional bone metabolism and blood flow at the lumbar spine measured by ^{18}F -fluoride positron emission tomography. *J Bone Miner Res* 2003; 18:2215-2222.
7. Doot RK, Muzi M, Peterson LM, et al. Kinetic analysis of ^{18}F -fluoride PET images of breast cancer bone metastases. *J Nucl Med* 2010;51:521-527.
8. Cook G Jr, Parker C, Chua S, Johnson B, Aksnes AK, Lewington VJ. ^{18}F -fluoride PET: changes in uptake as a method to assess response in bone metastases from castrate-resistant prostate cancer patients treated with ^{223}Ra -chloride (Alpharadin). *EJNMMI Res* 2011;1:4.

9. Nam S, Kim D, Cheng JQ, et al. Action of the Src family kinase inhibitor, dasatinib (BMS-354825), on human prostate cancer cells. *Cancer Res* 2005;65:9185–9189.
10. Fizazi K. The role of Src in prostate cancer. *Ann Oncol* 2007;18:1765–1773.
11. Summy JM, Gallick GE. Src family kinases in tumor progression and metastasis. *Cancer Metastasis Rev* 2003;22:337–358.
12. Myoui A, Nishimura R, Williams PJ, et al. C-SRC tyrosine kinase activity is associated with tumor colonization in bone and lung in an animal model of human breast cancer metastasis. *Cancer Res* 2003;63:5028–5033.
13. Rucci N, Recchia I, Angelucci A, et al. Inhibition of protein kinase c-Src reduces the incidence of breast cancer metastases and increases survival in mice: implications for therapy. *J Pharmacol Exp Ther* 2006;318:161–172.
14. Koreckij T, Nguyen H, Brown LG, Yu EY, Vessella RL, Corey E. Dasatinib inhibits the growth of prostate cancer in bone and provides additional protection from osteolysis. *Br J Cancer* 2009;101:263–268.
15. Yu EY, Wilding G, Posadas M, et al. Phase 2 study of dasatinib in patients with metastatic castration-resistant prostate cancer. *Clin Cancer Res* 2009;15:7421-7428.
16. Yu EY, Massard C, Gross M, et al. Once-daily dasatinib: Expansion of a phase 2 study evaluating the safety and efficacy of dasatinib in patients with metastatic castration-resistant prostate cancer. *Urology* 2011;77:1166-1171.

17. Araujo JC, Mathew P, Armstrong AJ, et al. Dasatinib combined with docetaxel for castration-resistant prostate cancer: results from a phase 1-2 study. *Cancer* 2012;118:63-71.
18. Araujo JC, Trudel GC, Saad F, et al. Randomized, double-blind, placebo-controlled phase 3 trial of docetaxel and dasatinib in men with metastatic castration-resistant prostate cancer. *Lancet Oncol* 2013;14:1307-1316.
19. Mendiratta P, Mostaghel E, Guinney J, et al. Genomic strategy for targeting therapy in castration-resistant prostate cancer. *J Clin Oncol* 2009;27:2022–2029.
20. Scher HI, Halabi S, Tannock I, et al. Design and end points of clinical trials for patients with progressive prostate cancer and castrate levels of testosterone: recommendations of the Prostate Cancer Clinical Trials Working Group. *J Clin Oncol* 2008;26:1148–1159.
21. Inoue S, Branch CD, Gallick GE, Chada S, Ramesh R. Inhibition of Src kinase activity by Ad-mda7 suppresses vascular endothelial growth factor expression in prostate carcinoma cells. *Mol Ther* 2005;12:707-715.
22. Lee YC, Huang CF, Murshed M, et al. Src family kinase/abl inhibitor dasatinib suppresses proliferation and enhances differentiation of osteoblasts. *Oncogene* 2010; 29:3196-3207.
23. Ryan CJ, Shah S, Efstathiou E, et al. Phase II study of abiraterone acetate in chemotherapy-naive metastatic castration-resistant prostate cancer displaying bone flare discordant with serologic response. *Clin Cancer Res* 2011;17:4854-4861.

24. Dancey JE, Dodd LE, Ford R, et al. Recommendations for the assessment of progression in randomised cancer treatment trials. *Eur J Cancer* 2009;45:281-289.
25. Roudier MP, True LD, Higano CS, et al. Phenotypic heterogeneity of end-stage prostate carcinoma metastatic to bone. *Hum Pathol* 2003;34:646-653.
26. Shah RB, Mehra R, Chinnaiyan AM, et al. Androgen-independent prostate cancer is a heterogeneous group of diseases: lessons from a rapid autopsy program. *Cancer Res* 2004;64:9209-9216.

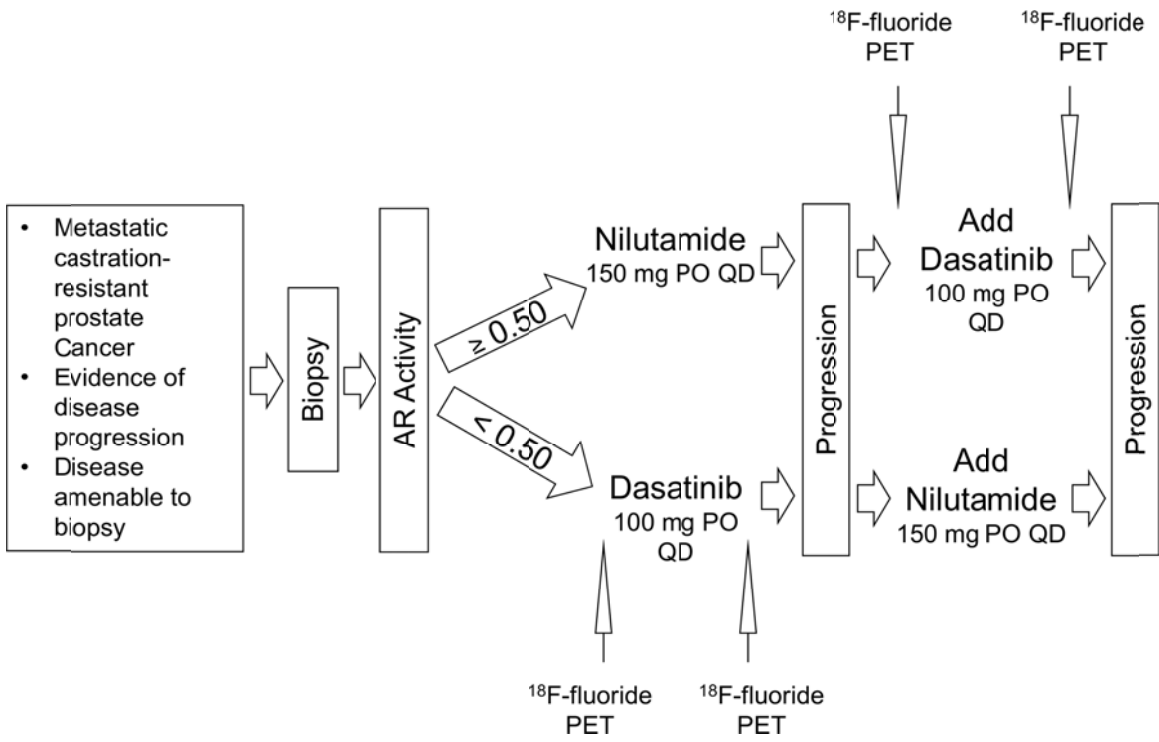
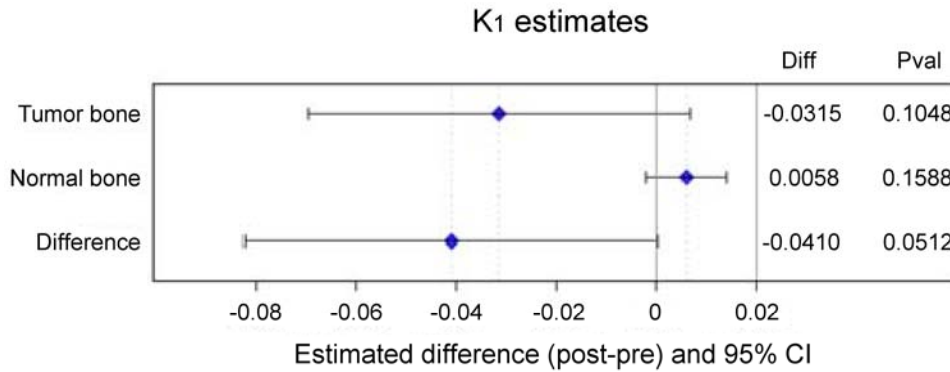
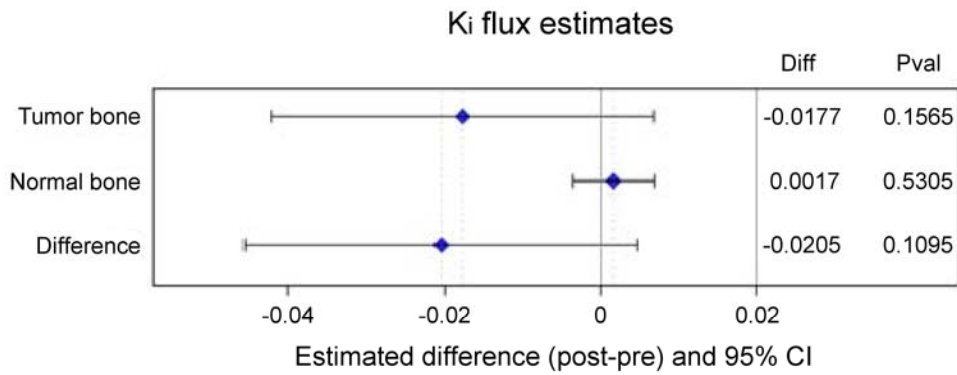
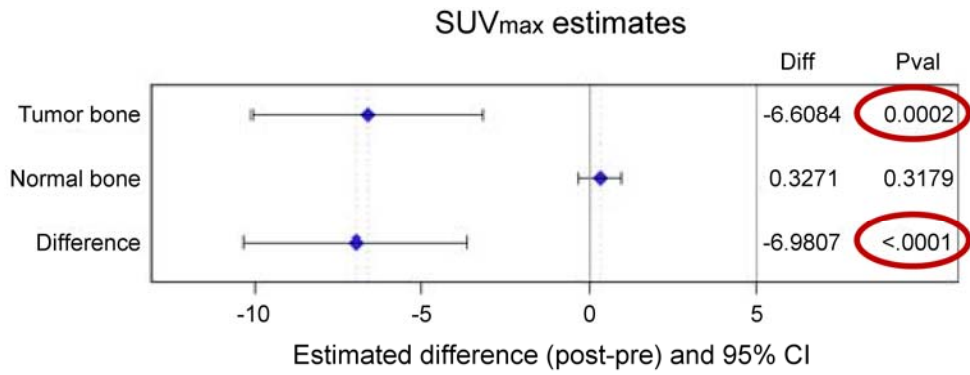


Figure 1. ^{18}F -fluoride PET was obtained at baseline prior to therapeutic introduction of dasatinib and 12 +/-4 weeks into therapy.



*Difference = Δ in tumor bone - Δ in normal bone

Figure 2. Change in regional fluoride incorporation occurred in response to dasatinib treatment in CRPC bone metastases when measured by SUV_{maxavg} but not by K_{1avg}. No significant changes were seen in response to dasatinib in normal bone. No significant changes in transport (K₁) were observed after treatment with dasatinib.

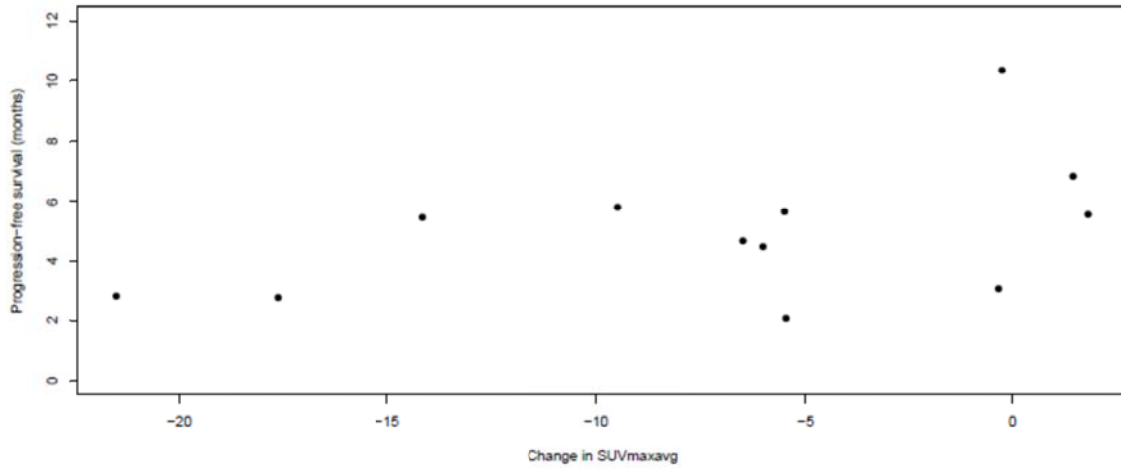


Figure 3. Individual patient changes in SUV_{maxavg} in response to treatment with dasatinib show less change correlates with longer PFS.

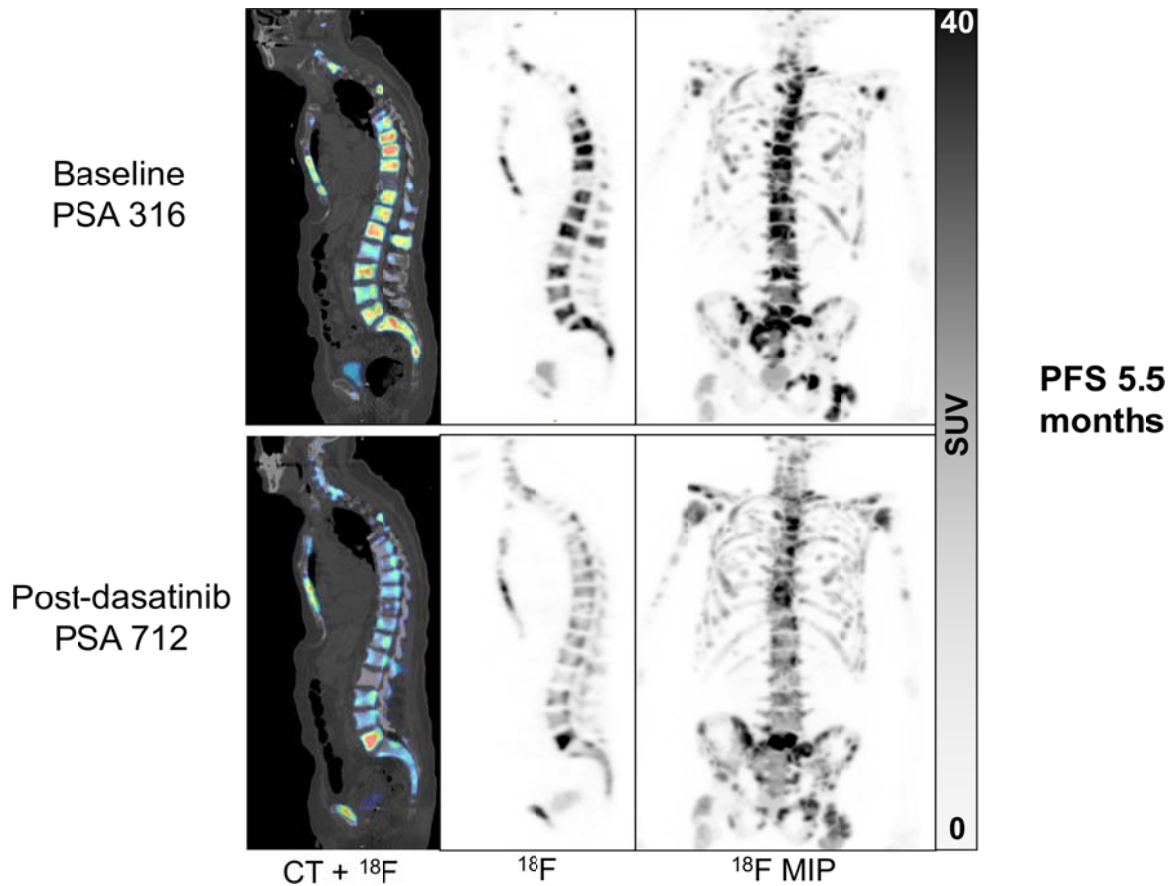


Figure 4. This patient had stable disease on bone and CT scan in response to dasatinib. Obvious heterogeneous changes in ^{18}F -fluoride PET response to dasatinib are detected, with decrease in ^{18}F -fluoride uptake in most bone metastases, yet the L5 lesion appears to have increased uptake.

TABLE 1. Patient demographics

Variable	Level	Evaluable Baseline PET scan n=17	Evaluable for Response to Treatment n=12
Age (yrs)	Median (range)	70 (48-86)	75 (58-86)
Primary Gleason score	Mean (SD)	4 (0.8)	4 (0.8)
PSA (ng/mL)	Mean (SD)	433 (1012)	235 (368)
Initial Treatment	Dasatinib	13	10
	Nilutamide	4	2
ECOG PS	0	12	9
	1	5	3
uNTX (nM/mmol Cr)	Mean (SD)	76 (104)	61 (76)
BAP (U/L)	Mean (SD)	60 (130)	20 (15)

TABLE 2. Univariate analysis for association with PFS.

Predictor	Baseline (n=17) or Δ (n=12) in response to dasatinib	HR/OR (95% CI)	P-Value
Gleason	Baseline	0.985(0.678-1.353)	0.81
PSA	Baseline	1.001 (1.000-1.001)	0.032
	Δ	1.002 (0.999-1.006)	0.23
uNTX	Baseline	1.008 (1.002-1.015)	0.013
	Δ	0.988 (0.965-1.011)	0.30
BAP	Baseline	1.006(1.001-1.011)	0.029
	Δ	1.009 (0.990-1.028)	0.35
SUV _{maxavg}	Baseline	1.006 (0.969-1.045)	0.75
	Δ	0.905 (0.816-1.002)	0.056
K _i	Baseline	51.930 (0.127-21,177.04)	0.20
	Δ	N/A*	N/A
K ₁	Baseline	1.376 (0.089-21.215)	0.82
	Δ	N/A*	N/A

* The models did not converge.

TABLE 3. Correlations (and p-values) between change of ¹⁸F-fluoride PET uptake parameters and change of PSA and bone biomarkers.

	SUV_{maxavg}	K_{iavg}	K_{1avg}	UNTX	BAP	PSA
SUV_{maxavg}	1.00	-	-	-	-	-
K_{iavg}	0.48 0.0024	1.00	-	-	-	-
K_{1avg}	0.43 0.0079	0.55 0.0004	1.00	-	-	-
uNTX	0.21 0.26	-0.14 0.47	-0.12 0.53	1.00	-	-
BAP	-0.58 0.0014	-0.052 0.80	-0.14 0.49	0.12 0.49	1.00	-
PSA	-0.12 0.47	0.12 0.49	-0.078 0.64	0.65 <.0001	0.20 0.22	1.00